

# Methane detection at 1670-nm band using a hollow-core photonic bandgap fiber and a multiline algorithm

A. M. Cubillas<sup>1\*</sup>, M. Silva-Lopez<sup>1</sup>, J. M. Lazaro<sup>1</sup>, O. M. Conde<sup>1</sup>, M. N. Petrovich<sup>2</sup> and J. M. Lopez-Higuera<sup>1</sup>

<sup>1</sup>Grupo de Ingeniería Fotónica, Dpto. TEISA, Universidad de Cantabria, Avda. Los Castros S/N, C.P. 39005 Santander, Spain

<sup>2</sup>Optoelectronics Research Centre, University of Southampton, Southampton SO17 1BJ, UK

\*Corresponding author: [cubillasam@unican.es](mailto:cubillasam@unican.es)

<http://gif.teisa.unican.es/>

**Abstract:** The long interaction pathlengths provided by hollow-core photonic bandgap fibers (HC-PBFs) are especially advantageous for the detection of weakly absorbing gases such as methane (CH<sub>4</sub>). In this paper, we demonstrate methane sensing with a 1670-nm band HC-PBF. A multiline algorithm is used to fit the R(6) manifold (near 1645 nm) and, in this way, to measure the gas concentration. With this method, a minimum detectivity of 10 ppmv for the system configuration was estimated.

©2007 Optical Society of America

**OCIS codes:** (060.2370) Fiber optics sensors; (230.3990) Microstructure devices; (300.1030) Absorption spectroscopy.

---

## References and Links

1. J.M. Lopez-Higuera, *Handbook of Optical Fibre Sensing Technology* (John Wiley & Sons New York, 2002).
2. T.A. Birks, P.J. Roberts, P.St.J. Russel, D.M. Atkin, T.J. Sheperd, "Full 2D photonic band gaps in silica/air structures," *Electron. Lett.* **31** 1941-1943 (1995).
3. R.F. Cregan, B.J. Mangan, J. C. Knight, T.A. Birks, P.St.J. Russel, P.J. Roberts, D.C. Allan, "Single-mode photonic band gap guidance of light in air," *Science* **285**, 1537-1539 (1999).
4. F. Benabid, "Hollow-core photonic bandgap fibre: new light guidance for new science and technology," *Phil. Trans. R. Soc. A* **364**, 3439-3462 (2006).
5. T. Ritari, J. Tuominen, H. Ludvigsen, J.C. Petersen, T. Sorensen, T.P. Hansen, H.R. Simonsen, "Gas sensing using air-guiding photonic bandgap fibers," *Opt. Express* **12**, 4080-4087 (2004).
6. L.W. Kornaszewski, N. Gayraud, J.M. Stone, W.N. MacPherson, A.K. George, J.C. Knight, D.P. Hand, D.T. Reid, "Mid-infrared methane detection in a photonic bandgap fiber using a broadband optical parametric oscillator," *Opt. Express* **15**, 11219-11224 (2007).
7. A.M. Cubillas, J.M. Lazaro, M. Silva-Lopez, O.M. Conde, M. Petrovich, J.M. Lopez-Higuera, High sensitive methane sensor based on a photonic bandgap fiber, Postdeadline EWOF'S'07 (2007).
8. J. Henningsen, J. Hald, J. C. Petersen, "Saturated absorption in acetylene and hydrogen cyanide in hollow-core photonic bandgap fibers," *Opt. Express* **13**, 10475-10482 (2005).
9. R. Thapa, K. Knabe, M. Faheem, A. Naweid, O.L. Weaver, K. L. Corwin, "Saturated absorption spectroscopy of acetylene gas inside large-core photonic bandgap fiber," *Opt. Lett.* **31**, 2489-2491 (2006).
10. J. Tuominen, T. Ritari, H. Ludvigsen, J.C. Petersen, "Gas filled photonic bandgap fibers as wavelength references," *Opt. Commun.* **255**, 272-277 (2005).
11. F. Couny, P.S. Light, F. Benabid, P.St.J. Russell, "Electromagnetically induced transparency and saturable absorption in all-fiber devices based on <sup>12</sup>C<sub>2</sub>H<sub>2</sub>-filled hollow-core photonic crystal fiber," *Opt. Commun.* **263**, 28-31 (2006).
12. B. Culshaw, G. Stewart, F. Dong, C. Tandy, D. Moodie, "Fibre optic techniques for remote spectroscopic methane detection," *Sens. Act. B* **51**, 25-37 (1998).
13. M. Gharavi, S.G. Buckley, "Diode laser absorption spectroscopy measurement of linestrengths and pressure broadening coefficients of the methane 2ν<sub>3</sub> band at elevated temperatures," *J. Mol. Spectrosc.* **229**, 78-88 (2005).
14. L. S. Rothman et al., "The HITRAN 2004 molecular spectroscopic database," *J. Quant. Spectrosc. Radiat. Transfer* **96**, 139-204 (2005).

15. V. Nagali and R.K. Hanson, "Design of a diode-laser sensor to monitor water vapour in high-pressure combustion gases," *App. Opt.* **36**, 9518-9527 (1997).
16. M.E. Webber, S. Kim, S.T. Sanders, D.S. Baer, R.K. Hanson and Y. Ikeda, "In situ combustion measurements of CO<sub>2</sub> by use of a distributed-feedback diode-laser sensor near 2.0 μm," *App. Opt.* **22**, 821-828 (2001).

## 1. Introduction

Diode laser-based absorption sensors are attractive for gas detection because its specific advantages such as high spectral resolution, precise gas species identification and possibility of remote and distributed measurements [1]. Hollow-core photonic bandgap fibers (HC-PBFs) have unique properties that make them suitable for gas sensing [2-4]. When the hollow core of the fiber is filled with gas, long interaction lengths between light and the gas confined in the core are achieved, thus enabling sensitive devices. Furthermore, HC-PBFs are particularly interesting for their possibilities of integrability and compactness. For these reasons, in the past few years, HC-PBFs have been investigated in applications such as gas detection [5-7], saturated absorption spectroscopic experiments [8,9], wavelength locking [10] and nonlinear-optics [11].

Detecting methane (CH<sub>4</sub>) is of special relevance in many industrial and safety applications. For gas detection, spectral sensors preferably address the strongest absorption lines. For methane, these are found in the mid-infrared spectrum around 3300 nm. Unfortunately, light sources and detectors in this region are expensive and cumbersome to operate. Recently, methane sensing using HC-PBFs has been carried out in this region [6]. A detection limit of 5% methane in air was reported in this band. Alternatively, in the near infrared region, sources and detectors are available at low-cost. In this region, methane has the strongest band, 2ν<sub>3</sub>, at 1670 nm. Commercial fibre optic methane sensors based on conventional absorption gas cells have been developed in this range [12]. However, HC-PBFs were not available in this wavelength range up to very recent times and gas sensing devices based on HC-PBFs were made in the weaker band of 1300 nm [5,7].

In this paper, we report, for the first time to our knowledge, the application of a 1670-nm band HC-PBF to the detection of methane. Particularly, we target the R(6) absorption line at 1645 nm (near 6077 cm<sup>-1</sup>) since it is the strongest feature in this region. This is a manifold of six transitions strongly broadened at our experimental conditions, hence overlapped in a single line. By fitting this profile with a multiline algorithm, the individual transitions lineshapes can be recovered. This technique has been validated by measuring the concentration of different methane samples. The sensitivity (minimum detection limit) of this arrangement is also estimated.

## 2. Theory

The absorbance of light through a gas,  $A_\nu$ , at a frequency  $\nu$  (cm<sup>-1</sup>) is related to the properties of the gas species through which the light is travelling by the Beer-Lambert law [1]. It can be expressed as:

$$A_\nu = -\ln\left(\frac{I_t}{I_o}\right) = k_\nu \cdot L \quad (1)$$

where the absorbance is related to the light transmitted through the gas,  $I_t$ , and the incident light,  $I_o$ ,  $k_\nu$  (cm<sup>-1</sup>) represents the spectral absorption coefficient and  $L$  (cm) the pathlength, i.e. the distance the light travels through the gas. The spectral absorption coefficient is given by [13]:

$$k_\nu = \sum_{i=1}^N P x S_i \phi_i(\nu - \nu_{0i}) \quad (2)$$

Here,  $N$  represents the number of transitions within a manifold,  $i$  a specific transition,  $P$  (atm) the total pressure of the medium,  $x$  the mole fraction of the gas species (related to the gas concentration),  $S_i$  ( $\text{cm}^{-2}\text{atm}^{-1}$ ) the linestrength for transition  $i$  and  $\phi_i(\nu - \nu_{0i})$  (cm) the lineshape function for transition  $i$  centered at  $\nu_{0i}$ .

The lineshape function is represented by a Gaussian profile when the effects of line broadening are due to thermal motion (Doppler broadening). The width of the lineshape is then described by the Doppler width,  $\Delta\nu_D$ . Alternatively, collision effects, due to pressure, give rise to a Lorentzian lineshape function (collisional broadening), characterized by the collisional width parameter,  $\Delta\nu_C$ . When both effects are significant, the resultant lineshape function is typically addressed using a Voigt profile.

### 3. Experimental setup

The HC-PBF used in our experiment was supplied by the Optoelectronics Research Centre at Southampton. The normalized transmission window for a 5.1-m-long fiber is illustrated in Fig. 1. The transmission bandgap sharply starts at 1375 nm and goes beyond 1700 nm (until 1850 nm according to specifications). This range is suitable for measuring the  $2\nu_3$  absorption band of methane at 1670 nm. The fiber has a core diameter of 12  $\mu\text{m}$ , composed of 7 missing cells, and an overall cross section of 230  $\mu\text{m}$  diameter, see inset. It has a loss of 100 dB/km and can be fabricated in  $\sim$ hundred meter lengths.

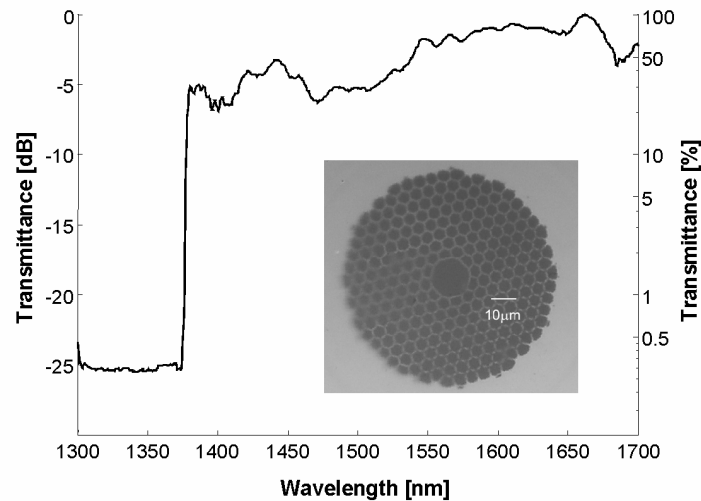


Fig. 1. Normalized spectral transmission of the HC-PBF used in the experiments. Shown in the inner panel is a microscope image of the fiber.

Figure 2 shows the experimental setup constructed for the detection of methane. Light from a tunable laser (Santec TSL-210V, spectral linewidth 1 MHz, i.e.  $3 \cdot 10^{-5} \text{ cm}^{-1}$ ) was launched into a single-mode fiber (SMF). The SMF was angle cleaved and coupled to one end of the 5.1-m-long HC-PBF. A gap was left between the SMF and HC-PBF to allow the gas access the hollow core of the fiber. The HC-PBF, with its open end, was placed inside a vacuum chamber. A pump was used to evacuate the air from the chamber and a pressure gauge monitored the pressure conditions in the chamber. The other end of the HC-PBF was spliced to a SMF and connected to a power meter (Agilent 8163A).

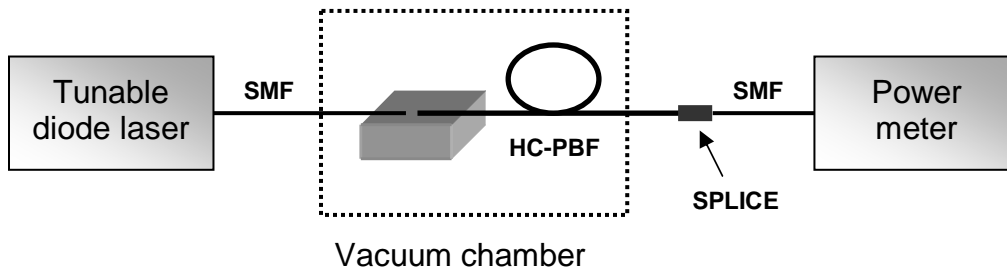


Fig. 2. Experimental setup for the detection of methane with a HC-PBF.

## 4. Results

### 4.1 Transmission spectrum of methane

Methane transmission spectrum was measured using the system described above. To obtain the  $2\nu_3$ -band transmission spectrum, the HC-PBF was filled with a calibrated concentration of 18750 ppmv (1.875%) methane in air at a relative pressure of 1 bar. The spectrum window was scanned with a resolution of 0.025 nm, with a wavelength range (1625-1680 nm) limited by the tunable source. The obtained spectrum, illustrated in Fig. 3, agrees with HITRAN database absorption lines [14]. R, Q and P branches at  $2\nu_3$  band are clearly seen and labelled in Fig. 3. Within these branches, every line is actually the overlapping resultant of a set of different transitions, a manifold, which can only be resolved at very low pressures. At higher pressures, collisional broadening produces overlapping of neighbouring energy transitions.

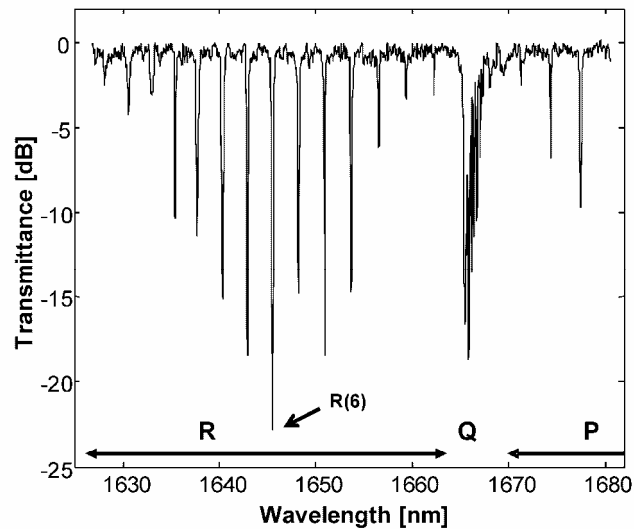


Fig. 3. Transmission spectrum of methane measured at room temperature and a relative pressure of 1 bar with a methane concentration of 18750 ppmv in air. The scanned resolution was 0.025 nm from 1625 nm to 1680 nm. P, Q and R branches are labelled. R(6) absorption line is also indicated.

### 4.2 Data analysis

As stated previously, for methane sensing purposes, a strong absorption line is required. We targeted the R(6) manifold at  $2\nu_3$  band, since it shows one of the best signal-to-noise ratios (SNR) (see Fig. 3). This manifold is comprised of six individual transitions, as listed in Table 1 [14].

Table 1. Individual transitions of the R(6) manifold<sup>a</sup>

Transition	$\nu_0$ (cm <sup>-1</sup> )	S (cm <sup>-2</sup> ·atm <sup>-1</sup> )
1	6076.928	1.192·10 <sup>-2</sup>
2	6076.935	1.899·10 <sup>-2</sup>
3	6076.954	3.000·10 <sup>-2</sup>
4	6077.028	1.768·10 <sup>-2</sup>
5	6077.046	1.847·10 <sup>-2</sup>
6	6077.063	3.050·10 <sup>-2</sup>
Manifold		1.276·10 <sup>-1</sup>

<sup>a</sup>From J. Quant. Spectrosc. Radiat. Transfer **96**, 139 (2005).

At our experimental conditions (room temperature, 1 bar of relative pressure), these transitions are strongly broadened and overlapped into a single spectral peak. For this reason, a multiline fit model, which takes into account all the transitions in the manifold, is used to both fit the manifold curve and recover the individual transition lineshapes. This fitting will allow us to estimate the methane concentration of the sample. At our pressure and temperature conditions, the effect of thermal broadening is negligible. Therefore, only broadening due to collisional effects ( $\Delta\nu_C$ ) will be taken into account. Thus, the lineshape function of the individual transitions will be Lorentzian [15]. In this way, and according to Eq. 2, to fit the R(6) absorption profile, three parameters per transition are necessary, i.e.  $S_i$ ,  $\Delta\nu_{Ci}$  and  $\nu_{0i}$ . The general form of the model for the R(6) manifold is described as follows:

$$A_\nu = PLx \sum_{i=1}^6 S_i \phi_i(\Delta\nu_{Ci}, \nu - \nu_{0i}) \quad (3)$$

Following the model used in [13], some simplifications can be considered in Eq. 3 to reduce the number of parameters. The collisional broadening is made equal for all the transitions in the manifold. Furthermore, at room temperature, the individual linestrengths of each transition,  $S_i$ , can be expressed in terms of the total linestrength of the manifold,  $S_{tot}$ , and a relative contribution,  $\omega_i$ , of each transition to the total linestrength. Moreover, the central frequency of each transition,  $\nu_{0i}$ , can be represented using an arbitrary central frequency,  $\nu_0$ , plus the wavenumber spacing of each transition  $i$  from  $\nu_0$ ,  $\delta\nu_i$ , as follows:

$$\nu_{0i} = \nu_0 + \delta\nu_i \quad (4)$$

Both  $\omega_i$  and  $\delta\nu_i$  parameters are calculated from HITRAN database [14]. This yields to a 3-parameter model ( $S_{tot}$ ,  $\nu_0$ ,  $\Delta\nu_C$ ) to handle the overlapped transitions that comprise the R(6) manifold:

$$A_\nu = PLx \sum_{i=1}^6 S_{tot} \omega_i \phi_i(\Delta\nu_C, \nu - \nu_{0i}) \quad (5)$$

The absorbance of the R(6) manifold was determined from the measured transmitted intensity and the incident intensity, using Eq. 1. These data points are plotted in Fig. 4 (upper). They were obtained using a 18750 ppmv (1.875%) sample of methane in air at room temperature and a relative pressure of 1 bar. The absorbance measurements were then non-linear least-squared fitted with a Levenberg-Marquardt algorithm using the model described in Eq. 5. The resultant 6-line Lorentzian fit is represented as a solid curve. The residuals (bottom) are calculated as the difference between the data and the curve fit. As can be observed, the fit and the data show a close correspondence. This Lorentzian fit provides the values of the three parameters of the model ( $S_{tot}$ ,  $\nu_0$ ,  $\Delta\nu_C$ ), which are later used to obtain the

gas concentration. The contributions from the individual transitions are also illustrated as broken curves.

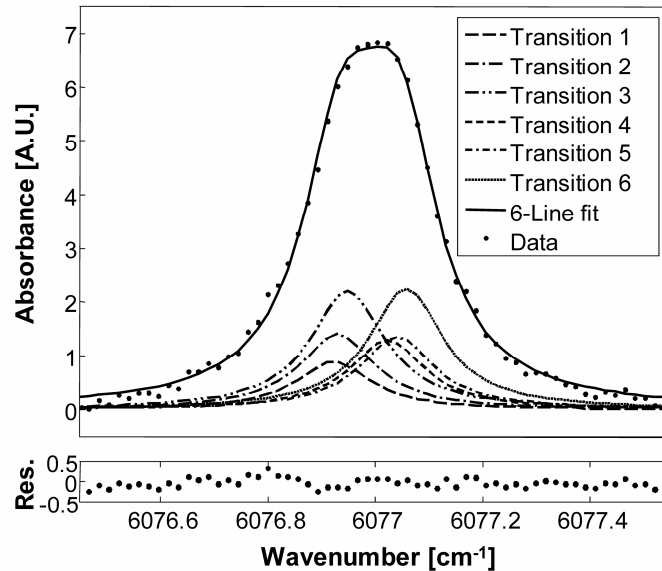


Fig. 4. 6-Line best Lorentzian fit (solid curve) for R(6) manifold near  $6077 \text{ cm}^{-1}$  at  $T=296\text{K}$ , relative pressure of 1 bar and methane concentration of 18750 ppmv (upper). Dots representing the experimental points and broken lines the contributions of each of the six transitions of the R(6) absorption line. The residual (bottom) is calculated as the difference between the data (dots) and the multiline best-fit Lorentzian profile (solid curve).

To validate this technique, the multiline algorithm presented before is applied to determine the concentration of methane for a set of different calibrated methane samples. Using the three parameters obtained in the fit, the concentration  $x$  is deduced from Eq. 5. In Fig. 5, a set of recovered measurements (dots) of methane concentration are plotted against the calibrated concentrations (solid line). As can be deduced, there is a good agreement between the experimental results and the calibrated samples. The repeatability of the experiment is also demonstrated.

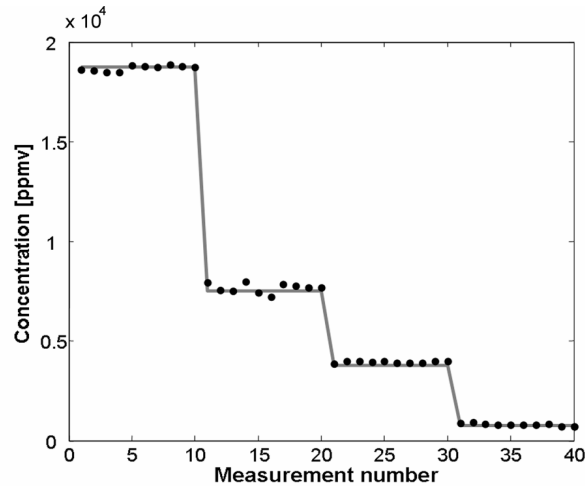


Fig. 5. Concentration measurements of methane estimated with the 6-line fit algorithm. Dots representing the experimental points and solid curve the calibrated methane concentration.

Finally, the sensitivity of the system was evaluated. The HC-PBF was filled with a concentration of 750 ppmv (0.075%) of methane in air at a relative pressure of 1 bar and the curve fitting of the R(6) feature was performed using the procedure described before. Etalon fringes due to unwanted reflections at the open end of the HC-PBF were present but were reduced by averaging 10 samples. As shown in Fig. 6, a SNR of 75 was obtained, which gives rise to a detection limit of 10 ppmv. That implies that, with our arrangement, a minimum detectable absorbance of  $8 \times 10^{-4}$  can be measured, which is very close to the typical performance of direct absorption spectroscopy schemes [16].

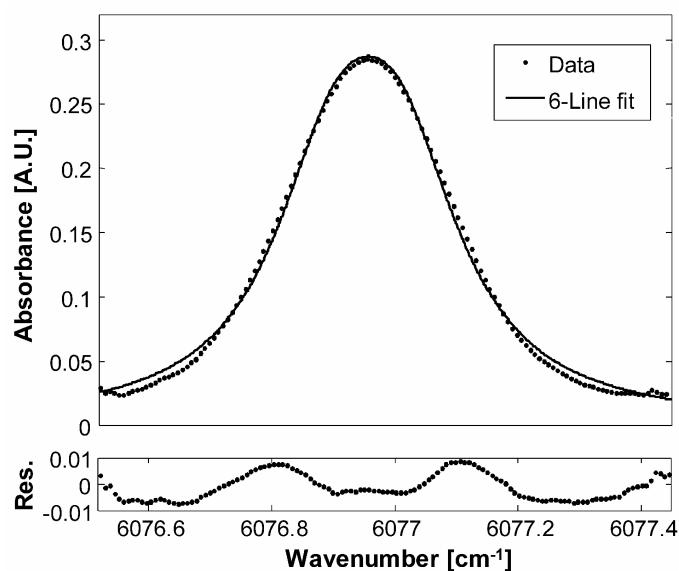


Fig. 6. 6-Line best Lorentzian fit for the R(6) manifold near  $6077 \text{ cm}^{-1}$  at  $T=296\text{K}$ , relative pressure of 1 bar and methane concentration of 750 ppmv (upper) and residual (bottom) used for the determination of the detection limit of the system.

## 5. Conclusions

In this paper we have presented, to our knowledge, the first application of a 1670-nm band HC-PBF to the detection of methane. This band, despite having relatively weak absorbing lines, benefits from the long pathlengths achievable with HC-PBF technology. The R(6) absorption line (near 1645 nm) was targeted because it showed a good SNR in the band. At our experimental conditions, collisional broadening made impossible the identification of the individual transitions within the R(6) absorption line. Thus, we applied a multiline model to fit the manifold. The fit allows to infer the methane concentration in air with an estimated detection limit of 10 ppmv. It also simulates the lineshape functions of the individual transitions that comprise the manifold. Furthermore, we believe that a more sensitive technique, such as a modulation scheme, could yield to a lower detection limit. Finally, further research is still needed in order to speed up the gas diffusion through the fiber.

## Acknowledgments

The authors acknowledge financial support for this work provided by the Spanish Government's Ministry of Science and Technology via the TEC'2004-05936-C02-02 and TEC'2005-08218-C02-02 projects. We also thank Prof. Rebollo, from the University of Zaragoza, for his assistance with the arc fusion splicing procedure.